# Flux Observer Algorithms for Direct Torque Control of Brushless Doubly-Fed Reluctance Machines

Hamza Chaal and Milutin Jovanovic
Northumbria University, School of Computing, Engineering and Information Sciences
Newcastle upon Tyne NE1 8ST, United Kingdom
E-mail: hamza.chaal@northumbria.ac.uk; milutin.jovanovic@northumbria.ac.uk

***Abstract*—Direct Torque Control (DTC) has been extensively researched and applied to most AC machines during the last two decades. Its first application to the Brushless Doubly-Fed Reluctance Machine (BDFRM), a promising cost-effective candidate for drive and generator systems with limited variable speed ranges (such as large pumps or wind turbines), has only been reported a few years ago. However, the original DTC scheme has experienced flux estimation problems and compromised performance under the maximum torque per inverter ampere (MTPIA) conditions. This deficiency at low current and torque levels may be overcome and much higher accuracy achieved by alternative estimation approaches discussed in this paper using Kalman Filter (KF) and/or Sliding Mode Observer (SMO). Computer simulations accounting for real-time constraints (e.g. measurement noise, transducer DC offset etc.) have produced realistic results similar to those one would expect from an experimental setup.**

***Index Terms*—Direct Torque Control, Kalman Filter, Sliding Mode Observer, Robust Exact Differentiator, Brushless Doubly-Fed Reluctance Machine.**

## NOMENCLATURE

$v_{pd}$, $v_{pq}$ primary direct and quadrature voltage components [V];
$v_{sd}$, $v_{sq}$ secondary direct and quadrature voltage components [V];
$i_{pd}$, $i_{pq}$ primary direct and quadrature current components [A];
$i_{sd}$, $i_{sq}$ secondary direct and quadrature current components [A];
$\lambda_{pd}$, $\lambda_{pq}$ primary direct and quadrature flux components [Wb];
$\lambda_{sd}$, $\lambda_{sq}$ secondary direct and quadrature flux components [Wb];
$\omega$ angular velocity of reference frame [rad/sec];
$\omega_{rm}$ mechanical angular velocity of the shaft [rad/sec];
$\omega_r$ electrical angular velocity of the rotor [rad/sec];
$\omega_{p,s}$ primary and secondary winding frequencies [rad/sec];
$P_r$ number of rotor poles (or the sum of the windings pole pairs);
$L_p$, $L_s$, $L_m$ primary, secondary and mutual 3-phase inductances of the windings [H];
$R_p$, $R_s$ primary and secondary windings resistances [$\Omega$];
$T_e$, $T_l$ electromagnetic and load torque [Nm].

## I. INTRODUCTION

The Brushless Doubly Fed Reluctance Machine (BDFRM) has been investigated during the last decade as a potential alternative to the existing solutions in variable speed applications with narrow speed ranges [1]–[8]. The main motivation for this increasing interest has been found in its modest cost and brushless structure as well as competitive performance relative to other self-cascaded counterparts i.e. the conventional doubly-excited wound rotor induction machine (DEWRIM) or a cage rotor cousin, the brushless doubly-fed induction machine (BDFIM) [9], [10]. As a member of the slip-power recovery family of machines, the BDFRM allows the use of a partially-rated inverter which, for a typical speed range of $2:1$ in pump drives or wind turbines [3], [8], may be rated up to about $25\%$ of the machine rating [1]–[3].

Apart from economic benefits, another interesting feature of the BDFRM is the operational mode flexibility. It can function as a slip ring induction machine (which represents an important "fail-safe" measure in case of the inverter failure) or as a wound rotor synchronous turbo-machine. The absence of rotor windings makes it more efficient [4] and easier to model/control compared to the BDFIM [3], whilst its brushless design ensures reliable, maintenance-free operation unlike the DEWRIM. The latter advantage may give preference to the BDFRM over the DEWRIM for off-shore wind turbines where operation and maintenance costs of brushed generators are significant. A further BDFRM merit, common with all doubly-fed machines, is the possibility of line power factor improvement. This property is particularly useful in weak networks but comes at the expense of increased inverter rating (and hence size) [8], [11], [12]. Note that in contrast to the BDFIM, the BDFRM and DEWRIM have inherently decoupled control of torque (real power) and reactive power [13].

The BDFRM has two standard, sinusoidally distributed stator windings of different applied frequencies and pole numbers. The primary or power winding is grid-connected, and the secondary or control winding is fed from a bi-directional (back-to-back) IGBT converter. In order to provide rotor position dependent magnetic coupling between the windings and torque production from the machine [2], [5], the reluctance rotor must have half the total number of stator poles. One implication of such unusual operating principle and unconventional design is the modest torque per volume so that a bigger BDFRM is needed to achieve the torque of an equivalent synchronous reluctance (SyncRel) or an induction machine [1]. Recent finite-element-analysis (FEA) studies have shown that with a rising rotor saliency-ratio, the BDFRM overall performance can potentially be improved (as with the SyncRel) [1] to a level competitive with the induction machine [14].

The fundamental DTC algorithm has been developed more than two decades ago [15] as a viable alternative to space vector or field oriented control for high-performance induction motor drives. Since then the method has gained enormous popularity in academic and industrial research communities

978-1-4244-4649-0/09/$25.00 ©2009 IEEE

due to its stator frame based hysteresis-type of flux and torque control without co-ordinate transformations. This property has made the DTC largely machine parameter independent (and hence versatile), conceptually simple and computationally effective offering high control rates and fast transient response to the machine. For instance, ABB® has adopted this control approach in a range of products for high speed applications such as traction or servo systems. However, while the literature is overwhelmed with DTC papers on various singly-excited machines, until recently, proportionally little work on this subject has been published for doubly-fed machines in general.

DTC has been successfully applied to the BDFRM either with [6], [16] or without [8], [12] a shaft position sensor for speed control. The voltage integration problems and associated flux estimation errors of cage induction machines at low supply frequencies [15], have been avoided in a modified DTC scheme proposed and simulated in [16] and experimentally verified in [6], [8], [12]. In this DTC concept, the secondary flux has been identified analytically through primary quantities of fixed line frequency and not using the secondary voltage measurements as in the traditional method but at the expense of having to know the windings self inductances. The DTC algorithm has been shown to perform very well even in speed sensor-less mode down to zero secondary frequency at unity power factor when the secondary magnetizing currents are larger [8], [12]. However, at low secondary currents, as is the case under maximum torque per inverter ampere (MTPIA) conditions, the flux estimator has exhibited pronounced sensitivity to parameter knowledge inaccuracies, preventing the control objective to be fulfilled in real-time [6].

The main purpose of this paper is to make a step forward toward overcoming the above limitation by conducting a comparative study of flux estimation techniques capable of providing more accurate estimates and therefore offering potential MTPIA performance improvement of the DTC.

## II. Dynamic Model

In an arbitrary rotating reference frame, the BDFRM $dq$-model can be represented by the following set of equations using standard notation [5]:

$$\begin{cases} v_{pd} = R_p i_{pd} + \dot{\lambda}_{pd} - \omega\lambda_{pq} \\ v_{pq} = R_p i_{pq} + \dot{\lambda}_{pq} + \omega\lambda_{pd} \\ v_{sd} = R_s i_{sd} + \dot{\lambda}_{sd} - (\omega_r - \omega)\lambda_{sq} \\ v_{sq} = R_s i_{sq} + \dot{\lambda}_{sq} + (\omega_r - \omega)\lambda_{sd} \end{cases} \tag{1}$$

$$\begin{cases} \lambda_{pd} = L_p i_{pd} + L_m i_{sd} \\ \lambda_{pq} = L_p i_{pq} - L_m i_{sq} \\ \lambda_{sd} = L_s i_{sd} + L_m i_{pd} \\ \lambda_{sq} = L_s i_{sq} - L_m i_{pq} \end{cases} \tag{2}$$

Among many equivalent torque expressions, the one best illustrating control principles is of the form:

$$T_e = \frac{3P_r L_m}{2L_p}\left(\lambda_{pd} i_{sq} + \lambda_{pq} i_{sd}\right) \tag{3}$$

In (3), the BDFRM torque is given as a function of the primary flux (which is virtually constant due to the primary winding grid connection) and controllable secondary currents. Therefore, torque control is achieved directly by varying the secondary current magnitudes through an inverter.

To complete the BDFRM model, a conventional mechanical equation, assuming a single lumped inertia load and neglecting friction components, has been used:

$$\frac{d\omega_{rm}}{dt} = \frac{1}{J}(T_e - T_l) \tag{4}$$

where the fundamental angular velocity relationship for the electro-mechanical energy conversion (i.e. torque production) in the machine is as follows:

$$\omega_{rm} = \frac{\omega_p + \omega_s}{P_r} \Longleftrightarrow n_{rm} = 60 \cdot \frac{f_p + f_s}{P_r} \tag{5}$$

## III. Flux Estimation using Kalman Filter

By manipulating (1) and (2) to eliminate the current variables, and referring the model to a stationary frame (i.e. $\omega = 0$), one obtains:

$$\begin{cases} \dot{\lambda}_{pd} = v_{pd} - \mu R_p(L_m\lambda_{sd} - L_s\lambda_{pd}) \\ \dot{\lambda}_{pq} = v_{pq} + \mu R_p(L_s\lambda_{pq} + L_m\lambda_{sq}) \\ \dot{\lambda}_{sd} = v_{sd} + \omega_r\lambda_{sq} - \mu R_s(L_m\lambda_{pd} - L_p\lambda_{sd}) \\ \dot{\lambda}_{sq} = v_{sq} - \omega_r\lambda_{sd} + \mu R_s(L_m\lambda_{pq} + L_p\lambda_{sq}) \end{cases} \tag{6}$$

where: $\mu = (L_m^2 - L_p L_s)^{-1}$.

It is clear that (6) represents a bilinear system of equations. However, a physical constraint is imposed on the BDFRM given that it offers cost advantages only in applications with a narrow speed range around the synchronous speed. For a typical speed range of 2:1 i.e. $\omega_{rm}^{max} = 2\omega_{rm}^{min}$, and $f_p = 50$ Hz, $f_s = \frac{f_p}{3} \approx 17$ Hz according to (5). Therefore, in the range $n_{rm} = n_{syn} \pm 250$ rpm, the power electronics required should only be rated at $20\%$ of the BDFRM rating [3]. This operating limit can be exploited to simplify estimation and/or control schemes. In fact, since $\omega_r = P_r\omega_{rm}$, then $\omega_r$ also exhibits the same uncertainty as $\omega_{rm}$. Assuming a constant nominal electrical velocity $\omega_r = \omega_n$, the KF system model becomes of standard linear form:

$$\dot{X} = AX + BU \tag{7}$$

where: $X = \begin{bmatrix}\lambda_{pd} & \lambda_{pq} & \lambda_{sd} & \lambda_{sq}\end{bmatrix}^T$, $B = I_{4\times4}$, $U = \begin{bmatrix}v_{pd} & v_{pq} & v_{sd} & v_{sq}\end{bmatrix}^T$, and

$$A = \begin{bmatrix} \mu R_p L_s & 0 & -\mu R_p L_m & 0 \\ 0 & \mu R_p L_s & 0 & \mu R_p L_m \\ -\mu R_s L_m & 0 & \mu R_s L_p & \omega_n \\ 0 & \mu R_s L_m & -\omega_n & \mu R_s L_p \end{bmatrix}.$$

The machine currents are measured quantities, so one can rewrite (2) to get the output in the form $Y = CX$:

$$\begin{bmatrix} i_{pd} \\ i_{pq} \\ i_{sd} \\ i_{sq} \end{bmatrix} = \mu \begin{bmatrix} -L_s & 0 & L_m & 0 \\ 0 & -L_s & 0 & -L_m \\ L_m & 0 & -L_p & 0 \\ 0 & -L_m & 0 & -L_p \end{bmatrix} \begin{bmatrix} \lambda_{pd} \\ \lambda_{pq} \\ \lambda_{sd} \\ \lambda_{sq} \end{bmatrix} \tag{8}$$

To obtain a discrete model, the Euler's method with a sampling time $h$ can be applied to give:

$$\begin{cases} X_{k+1} = A_k X_k + hBU_k + \xi \\ Y_k = CX_k + \eta \end{cases} \tag{9}$$

where: $A_k = \begin{bmatrix} a_1 & 0 & a_3 & 0 \\ 0 & a_1 & 0 & -a_3 \\ a_4 & 0 & a_2 & \omega_n h \\ 0 & -a_4 & -\omega_n h & a_2 \end{bmatrix}$, $a_1 = 1+\mu R_p L_s h$, $a_2 = 1+\mu R_s L_p h$, $a_3 = -\mu R_p L_m h$, $a_4 = -\mu R_s L_m h$. $\xi$ and $\eta$ are introduced to account for the process and measurement noises and are assumed identically independent zero mean white noises of covariance $Q$, $R$ respectively.

The KF equations are defined as follows [17]:

$$\begin{cases} \hat{X}_k = A_k \hat{X}_k + B_h U_k \\ P_k = A_k P_k A_k^T + Q_k \\ K_k = P_k C^T (C P_k C^T + R)^{-1} \\ \hat{X}_{k+1} = \hat{X}_k + K_k (Y_k - C\hat{X}_k) \\ P_{k+1} = (I - K_k C) P_k (I - K_k C)^T + K_k R K_k^T \end{cases} \tag{10}$$

where $K$ is the Kalman correction gain and $P$ is the state prediction covariance. Note that the last recursive equation in (10) may be simplified to $P_{k+1} = (I - K_k C)P_k$ as found in many texts. However, this approximation would be at the cost of numeric stability and accuracy of the original expression.

## IV. Flux Estimation using SMO

The application of Sliding Mode Observers (SMO) is relatively juvenile as the earliest contributions appeared in the late 1980s [18], [19]. A good survey on their development and applications can be found in [20]. The SMO design shares the same nominal model assumption as while developing the KF equations. Accordingly, the square linear uncertain system is defined by (7) and (8), where $A, B, C$ are of full rank.

Consider the coordinate transformation $x \mapsto Tx$, and select $T = C$. Then the transformed system is:

$$\begin{cases} \dot{X} = A_c X + B_c U \\ Y = C_c X \end{cases} \tag{11}$$

where: $A_c = TAT^{-1}$, $B_c = TB$, $C_c = CT^{-1} = I$.

The observer consists of a linear part (known as the Luenberger observer) and a non-linear term responsible for robust performance. It is defined by:

$$\begin{cases} \dot{\hat{X}} = A_c \hat{X} + B_c U + L(Y - \hat{Y}) + M sgn(Y - \hat{Y}) \\ \hat{Y} = \hat{X} \end{cases} \tag{12}$$

where $sgn(Y - \hat{Y}) = [sgn(\tilde{x}_1),\ sgn(\tilde{x}_2),\ sgn(\tilde{x}_3),\ sgn(\tilde{x}_4)]^T$ and $\tilde{X} = X - \hat{X}$. The error dynamics are:

$$\begin{aligned} \dot{X} - \dot{\hat{X}} &= A_c X + B_c U - [A_c \hat{X} + B_c U + L(Y - \hat{Y}) \\ &\quad + M sgn(Y - \hat{Y})] \\ \dot{\tilde{X}} &= (A_c - L)\tilde{X} - M sgn(\tilde{X}) \end{aligned} \tag{13}$$

Let $L$ be selected such that $A_1 = A_c - L$ is Hurwitz. Consider the candidate Lyapunov function $V = \tilde{X}^T P \tilde{X}$ where $P$ is a real symmetric positive definite matrix. Since $A_1$ is stable then a real symmetric positive definite matrix $Q$ exists such that $PA_1 + A_1^T P = -Q$. Therefore:

$$\begin{aligned} \dot{V} &= \tilde{X}^T P \frac{d\tilde{X}}{dt} + \frac{d\tilde{X}^T}{dt} P \tilde{X} \\ &= \tilde{X}^T P A_1 \tilde{X} - \tilde{X}^T P M sgn(\tilde{X}) \\ &\quad + \tilde{X}^T A_1^T P \tilde{X} - sgn^T(\tilde{X}) M^T P \tilde{X} \\ &= \tilde{X}^T (P A_1 + A_1^T P) \tilde{X} - 2\tilde{X}^T P M sgn(\tilde{X}) \\ &= -\tilde{X}^T Q \tilde{X} - 2\tilde{X}^T P M sgn(\tilde{X}) \end{aligned}$$

By choosing $M = P^{-1}$, then:

$$\begin{aligned} \dot{V} &= -\tilde{X}^T Q \tilde{X} - 2\tilde{X}^T sgn(\tilde{X}) \\ &< 0,\ \forall\ \tilde{X} \neq [0,0,0,0]^T. \end{aligned}$$

In summary, the SMO design procedure relies on coordinates mapping that transforms the system equations into a special form, determination of matrix $L$ by pole placement and an arbitrary choice of a positive definite matrix $M$.

## V. Comparative Analysis of Flux Estimators

### A. Conventional Estimation

Recall the stationary frame space-vector expressions used for the flux estimation in the DTC algorithm presented in [6]:

$$\underline{\lambda}_s = \lambda_s e^{j\theta_s} = L_s \underline{i}_s + \frac{\underline{\lambda}_p - L_p \underline{i}_p}{\underline{i}_s^*} \underline{i}_p^* \tag{14}$$

$$\underline{\lambda}_p = \lambda_p e^{j\theta_p} = \int \left(\underline{v}_p - R_p \underline{i}_p\right) dt \tag{15}$$

The main advantage of this approach is that the well-known voltage integration problems while estimating $\lambda_s$ and $\theta_s$ (for sector identification) are avoided. However, it is clear that (14) is not numerically reliable if $i_s$ is close to zero (which is the case, for example, when the machine is lightly loaded or unloaded). Furthermore, (15) and especially (14) are both sensitive to parameter knowledge inaccuracies [6]. Therefore, using (14) is not recommended for real-time implementation and a more accurate estimation technique is required.

### B. KF Estimator

The KF algorithm has been implemented using an Embedded Matlab function to automatically generate an efficient C code and run simulations at compiled C speed. The code has been optimized by minimizing the use of computationally time consuming functions and/or manipulations.

As a state observer, the KF has advantages over the estimation method used in [6]. The DTC performance for MTPIA strategy has been simulated using both the estimation techniques for comparison. The KF initial estimates have been set to zero, and the covariance matrices to $P = 10 \times I,\ Q = 0.001 \times I,\ R = 0.1 \times I$. The estimation errors of the secondary flux components are shown in Figs. 1 and 2. Similar results have been obtained for the primary flux estimates but are not shown here for space reasons.

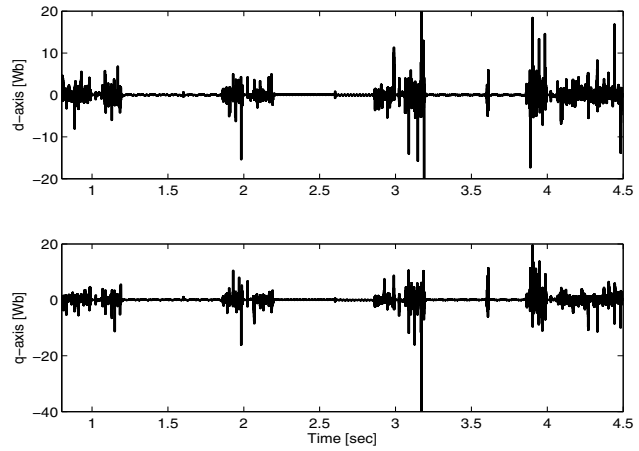


Fig. 1. Secondary flux estimation error using conventional method and ideal models

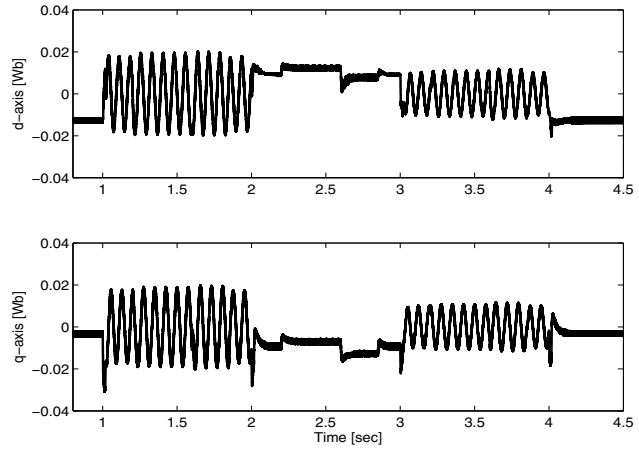


Fig. 2. Secondary flux estimation error using KF under ideal conditions

### C. Sliding Mode Observer (SMO)

The SM state observer (SMO) has been simulated under the same conditions as the KF. The matrix $L$ has been chosen to place eigenvalues of $A_1$ at $\{-4000, -4050, -4100, -4150\}$, and $M = diag([1\ 1\ 1\ 1])$. The estimation errors of the secondary flux components are depicted in Fig. 3. The SMO provides accurate estimates (up to about $2\%$) despite the changing speed and load set points. It is also simpler and computationally less demanding than the KF, which is a clear advantage when it comes to practical realization.

In order to illustrate the limitations of the conventional estimation method relative to its counterparts considered above, simulations in this section have been carried out under ideal circumstances. However, to be able to favor either of the proposed alternatives, a comparative performance evaluation of KF and SMO for a more realistic scenario is required.

## VI. Enhanced DTC

One of the necessary introductory steps to the experimental work is to make computer simulations as much real as possible. To this extent, the following actions have been taken: (1) The power electronic models from the Simulink/SimPowerSystems® library have been used; (2) High frequency uncorrelated white noises and unknown slowly varying DC offsets have been superimposed to the ideal signals to account for practical effects of measurement noise and current/voltage transducers; (3) It has been assumed that the only information available for the speed estimator is the rotor angular position provided by a shaft sensor.

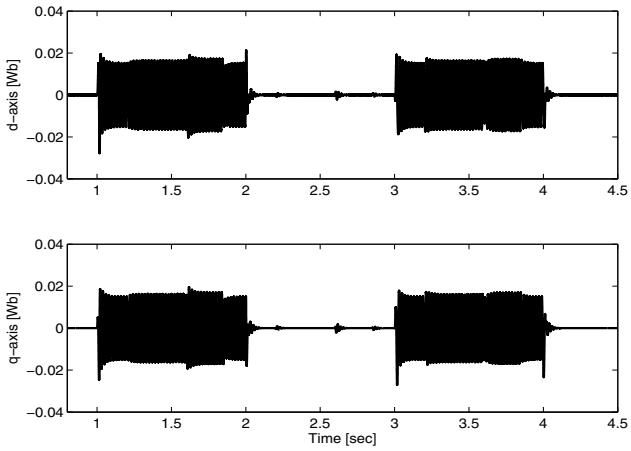


Fig. 3. Secondary flux estimation error using SMO for desired speed and load torque changes similar to those in Figs. 6 and 7

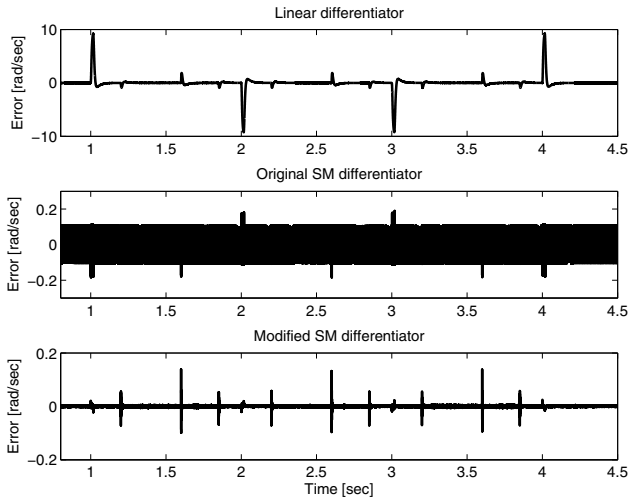


Fig. 4. Differentiation errors of rotor angular velocity estimates for speed and torque profiles as in Figs. 6 and 7

The classical way of obtaining the derivative of a physical measured quantity is to combine an ideal differentiator and a low-pass filter. Such a linear differentiator inherently carries a time-delay proportional to its complexity. A method for Robust Exact Differentiation (RED) based on Sliding Mode (SM) techniques has been introduced in [21] and adapted for the scope of this paper as described in [22]. Fig. 4 shows the results obtained by simulating the closed-loop DTC algorithm in [6] using a linear differentiator, the original RED [21] and the modified RED [22] for speed estimation. It is evident that the latter approach has half the maximum error of the original RED and as such is the most promising.

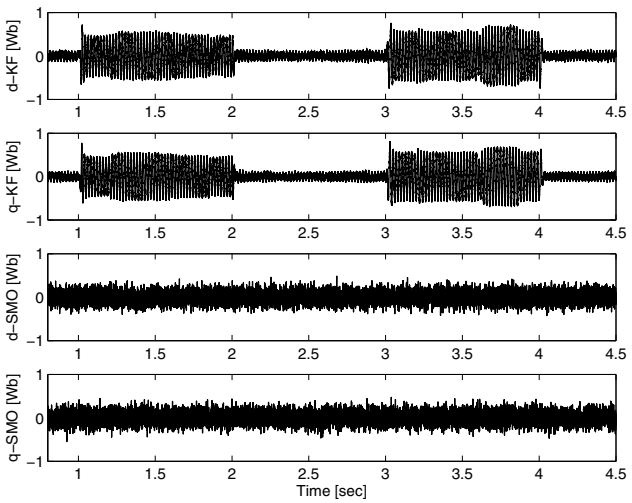


Fig. 5. KF and SMO secondary flux estimation errors using real models in simulations

### A. KF vs SMO Flux Estimation

The simulated estimation errors for KF and SMO appear in Fig.5. Notice that due to the inherent noise filtering ability, the KF offers the best estimates in the vicinity of synchronous speed when there is little mismatch between the KF and BDFRM models. However, moving away from the nominal conditions, the quality of KF estimates deteriorates although ideally this should not be the case according to Fig. 2. The sensitivity to parameter knowledge inaccuracies is the major KF drawback since the nonlinearities and measurement offset considered in this simulation scenario could be thought of as parameter uncertainties in the KF nominal model. Furthermore, despite the optimized coding, it would be difficult for a common DSP controller to handle real-time computations associated with the 4th order KF model which represents another practical limitation for high performance DTC.

On the other hand, the SMO provides uniform estimates irrespective of the operating mode, speed region or loading conditions of the BDFRM. The SMO has no information about the disturbance or uncertainties hence only a proper choice of $L, M$ matrices helps the observer to converge to the real state trajectory. However, there is a trade-off between the SMO robustness and its noise sensitivity. Increasing the magnitude of the discontinuous term enhances robustness to parameter uncertainties but at the cost of noisy estimates [18] (Fig.5). Low-pass pre-filtering would improve the SMO performance but this was not done for the sake of an objective comparison with the KF. The fact that the SMO is computationally effective, and that it doesn't suffer from the KF limitations stated above, makes it suitable for practical implementation.

### B. SMO based DTC

The response of the improved version of the DTC scheme in [6] to changes of desired speed and/or load torque has been investigated over the limited speed range of interest to the BDFRM target applications. Computer simulations have been conducted for a custom built 6/2-pole prototype using the parameters that can be found in [6], [16].

The BDFRM is usually started with the shorted secondary windings as a wound rotor induction machine. The BDFRM with a 4-pole rotor ($P_r = 4$) has the synchronous speed of $n_{syn} = 750$ rpm according to (5) for $f_p = 50$ Hz and $f_s = 0$ when the secondary winding, emulating the field winding of a classical $2P_r$-pole synchronous machine, is DC fed. In the following figures, the starting waveforms have been omitted to focus on the doubly-fed operating mode.

Figs. 6 and 7 illustrate the good tracking performance of the closed loop DTC in both speed regions (super-synchronous and sub-synchronous). The shaft angular velocity and machine torque accurately follow the desired trajectories with a ramp speed reference signal being introduced for smooth transients. The characteristic spikes in Fig. 6 reflect the PI speed control response to step changes in load torque. Note from Fig. 7 that the torque waveform is subject to high jitter due to the simulated real-time effects and the adopted switching strategy using only active voltage vectors to eliminate speed dependence of the torque controller [6].

Fig. 8 depicts the corresponding secondary dq-currents where the magnetizing d-axis component is virtually zero for a given torque (confirming that the MTPIA control objective has been achieved) whereas the torque producing q-axis component is in perfect correlation with Fig.7 as expected.

Finally, the power results in Fig. 9 indicate the compromised primary power factor values which can be explained by the fact that the primary winding is entirely responsible for the machine magnetization under the MTPIA conditions [11].

## VII. Conclusion

In this paper, the existing DTC method for the BDFRM has been reviewed addressing the weaknesses of the dedicated flux estimation technique using the MTPIA control strategy allowing improved efficiency of the machine by minimizing the secondary current magnitude (and hence copper losses) for a given torque. To overcome the associated limitations, alternative estimator designs have been suggested and detailed. The comparative simulation studies taking into account the real-time effects have shown that the SMO based algorithm is the preferable choice owing to its superiority to the KF in terms of the intrinsic robustness to disturbances, parameter uncertainties and computational burden. The preliminary results have demonstrated the MTPIA performance improvement of the modified DTC scheme the experimental verification of which is currently in progress.

## Acknowledgment

The authors would like to thank the EPSRC (Grant No. EP/F06148X/1) for financial support.

## References

[1] R. E. Betz and M. G. Jovanovic, "The brushless doubly fed reluctance machine and the synchronous reluctance machine-a comparison," *IEEE Transactions on Industry Applications*, vol. 36, pp. 1103–1110, 2000.

[2] ——, "Theoretical analysis of control properties for the brushless doubly fed reluctance machine," *IEEE Transactions on Energy Conversion*, vol. 17, pp. 332–339, 2002.

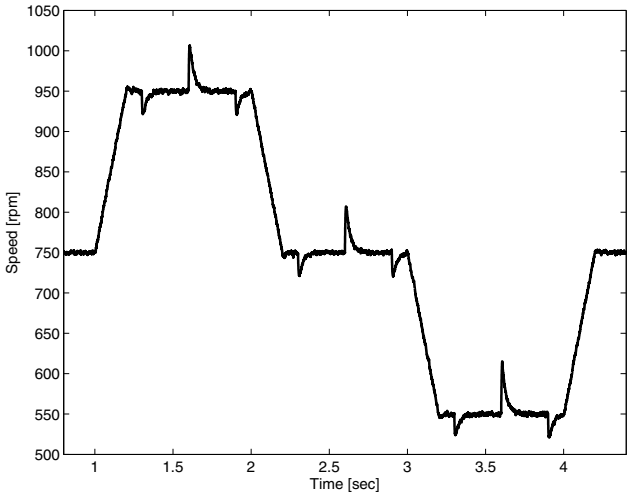


Fig. 6. Speed response under different loading conditions

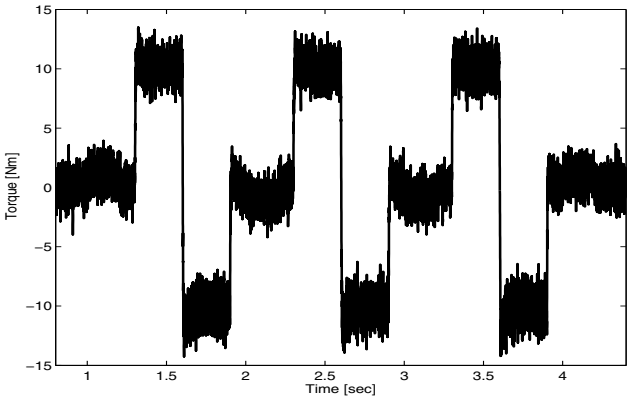


Fig. 7. Electromagnetic torque for the speed profile in Fig. 6

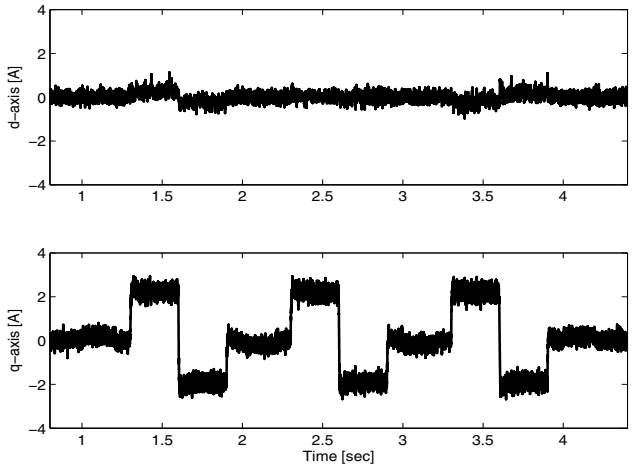


Fig. 8. Secondary current components in a flux oriented reference frame

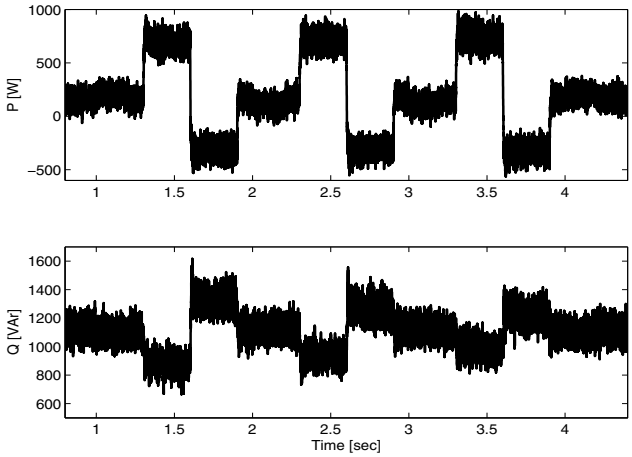


Fig. 9. Primary real and reactive powers


[3] M. G. Jovanovic, R. E. Betz, and J. Yu, "The use of doubly fed reluctance machines for large pumps and wind turbines," *IEEE Transactions on Industry Applications*, vol. 38, pp. 1508– 1516, 2002.

[4] F.Wang, F.Zhang, and L.Xu, "Parameter and performance comparison of doubly-fed brushless machine with cage and reluctance rotors," *IEEE Transactions on Industry Applications*, vol. 38, no. 5, pp. 1237–1243, Sept/Oct 2002.

[5] M. G. Jovanovic, R. E. Betz, and J. Yu, "Introduction to the space vector modelling of the brushless doubly-fed reluctance machine," *Electric Power Components and Systems*, vol. 31, no. 8, pp. 729–755, 2003.

[6] M. G. Jovanovic, J. Yu, and E. Levi, "Encoderless direct torque controller for limited speed range applications of brushless doubly fed reluctance motors," *IEEE Transactions on Industry Applications*, vol. 42, no. 3, pp. 712–722, 2006.

[7] F. V. Puleston, "Variable structure control of a wind energy conversion system based on a brushless doubly fed reluctance generator," *IEEE Transactions on Energy Conversion*, vol. 22, no. 2, pp. 499–506, 2007.

[8] D.G.Dorrell and M.Jovanović, "On the possibilities of using a brushless doubly-fed reluctance generator in a 2 MW wind turbine," *IEEE Industry Applications Society Annual Meeting (IAS)*, pp. 1–8, 5-9 October 2008.

[9] R.A.McMahon, P.C.Roberts, X.Wang, and P.J.Tavner, "Performance of BDFM as generator and motor," *IEE Proc.-Electr. Power Appl.*, vol. 153, no. 2, pp. 289–299, March 2006.

[10] J. Poza, E. Oyarbide, D. Roye, and M. Rodriguez, "Unified reference frame dq model of the brushless doubly fed machine," *IEE Proc.-Electr. Power Appl.*, vol. 153, no. 5, pp. 726–734, Sept 2006.

[11] M.G.Jovanović and R.E.Betz, "Power factor control using brushless doubly fed reluctance machines," *Proc. of the IEEE-IAS Annual Meeting*, vol. 1, pp. 523–530, Rome, Italy, October 2000.

[12] M.G.Jovanović and M.M.R.Ahmed, "Sensorless speed control strategy for brushless doubly-fed reluctance machines," *Electric Machines and Drives Conference (IEMDC)*, vol. 2, pp. 1514–1519, 3-5 May 2007.

[13] L. Xu, L. Zhen, and E. Kim, "Field-orientation control of a doubly excited brushless reluctance machine," *IEEE Transactions on Industry Applications*, vol. 34, no. 1, pp. 148–155, Jan/Feb 1998.

[14] E.M.Schulz and R.E.Betz, "Optimal torque per amp for brushless doubly fed reluctance machines," *Proc. of IEEE IAS Annual Meeting*, vol. 3, pp. 1749–1753, Hong Kong, October 2005.

[15] I. Takahashi and N. Toshihiko, "A new quick-response and high-efficiency control strategy of an induction motor," *IEEE Transactions on Industry Applications*, vol. 1A-22, no. 5, pp. 820–827, 1986.

[16] M.G.Jovanović, J.Yu, and E.Levi, "Direct torque control of brushless doubly fed reluctance machines," *Electric Power Components and Systems*, vol. 32, no. 10, pp. 941–958, October 2004.

[17] Y. Bar-Shalom, X. R. Li, and T. Kirubarajan, *Estimation with Applications to Tracking and Navigation: Theory Algorithms and Software*, 1st ed. Wiley-Interscience, 2001.

[18] J.-J. Slotine, J. Hedrick, and E. Misawa, "On sliding observers for nonlinear systems," *Proceedings of the American Control Conference*, pp. 1794–1800, 1986.

[19] B. Walcott, M. Corless, and S. Zak, "Comparative study of non-linear state-observation techniques," *International Journal of Control*, vol. 45, no. 6, pp. 2109–2132, 1987.

[20] S. K. Spurgeon, "Sliding mode observers: A survey," *International Journal of Systems Science*, vol. 39, no. 8, pp. 751–764, 2008.

[21] A. Levant, "Robust exact differentiation via sliding mode technique," *Automatica*, vol. 34, pp. 379–384, 1998.

[22] H. Chaal and M. Jovanovic, "Improved direct torque control using kalman filter: Application to a doubly-fed machine," *The 11th IASTED Int. Conf. on Control and Applications*, Cambridge, UK, July 2009.